Electronic Supplementary Information (ESI)

for

Magnetic-Graphitic-Nanocapsule Templated Diacetylene Assembly and Photopolymerization for Sensing and Multicoded Anti-counterfeiting

Xiang-Kun Nie,[a] Yi-Ting Xu,[a] Zhi-Ling Song,[a] Ding Ding,[a] Feng Gao,[c] Hao Liang,[a] Long Chen,[d] Xia Bian,[a] Zhuo Chen, *[,a] and Weihong Tan *[, a,b]

[a] Molecular Science and Biomedicine Laboratory, State Key Laboratory of Chemo/Bio-Sensing and Chemometrics, College of Chemistry and Chemical Engineering, College of Biology, Hunan University, Changsha, 410082, China.

[b] Department of Chemistry and Department of Physiology and Functional Genomics, Center for Research at Bio/nano Interface, Shands Cancer Center, UF Genetics Institute and McKnight Brain Institute, University of Florida, Gainesville, Florida 32611-7200, United States.

[c] Department of Radiology, The Third Xiangya Hospital of Central South University, Changsha, 410013, China.

[d] Faculty of Sciences, University of Macau, Av. Padre Tomás Pereira Taipa, Macau, China.

E-mail: zhuochen@hnu.edu.cn, tan@chem.ufl.edu

*To whom correspondence should be addressed.

1. Experimental Details

Selected area electron diffraction characterization of MGN@PDAs.

We identified a crystalline body-centered cubic FeCo core for the MGN@PDAs by selected area electron diffraction (Figure. S1). The diffraction patterns in the electron diffraction can be assigned to the (002) facets of the hexagonal crystalline graphite, the (110), (200) and (211) facets of the body-centered cubic structures of FeCo crystal, respectively.

Dynamic light scattering characterization of MGN@PDAs.

The hydrodynamic diameters of the MGN@PDAs under investigation were measured using a Zetasizer Nano ZS90 DLS system equipped with a red (633 nm) laser and an Avalanche photodiode detector (APD) (quantum efficiency > 50% at 633 nm) (Malvern Instruments Ltd., Worcestershire, England). DLS measurements were performed at room temperature at a fixed scattering angle of 90°. Figure. S2 shows the size distribution of the suspended MGN@PDAs. The average size was around 15 nm, which agreed with the size measured from the TEM. All size distributions reported here were based on number counting. The average particle size was obtained using a non-negative least-squares (NNLS) analysis method. For each sample, two DLS measurements were conducted with a fixed 10 runs, and each run lasted 10 s.

ζ-potential measurement of MGN@PDAs.

ζ-potential measurements were performed in water. The measurements were carried out at room temperature on the ZetaSizer Nano ZS90 equipped with a MPT-2 Autotitrator and a 4 mW He−Ne Laser (λ_0 = 633 nm), using the Laser Doppler Electrophoresis technique. The ζ-potential was calculated by Dispersion Technology software provided by Malvern according to the Smoluchowski approximation in an automatic mode. Figure. S3 shows the ζ-potential curves of the MGN@PDAs

water solution. The negative charge of the MGN@PDAs originated from the carboxyl groups of the PDA molecules.

Optimization of the fabrication of MGN@PDAs.

To fabricate the water-soluble and stable MGN@PDAs with high fluorescence signal, optimization of the MGN over PCDA concentration ratio was explored. UV-Vis was utilized to characterize the assembly efficiency of the PDAs on the MGN surface. The absorbances around 694 nm and 808 nm were used to represent the concentration of the PDAs and MGN, respectively. As shown in Figure. S4, after the concentration ratio of the PCDA over MGN was larger than three, the I_{694}/I_{808} reached a plateau, which indicated saturation of the PCDA molecules assembled on the MGN surface. The optimized concentration ratio of 3 was then fixed for all later experiments.

Thermo-responsive property of the MGN@PDAs

The MGN@PDAs complex is thermo-responsive, because heating disturbs the hydrogen bonds in the MGN@PDAs and induces changes in fluorescence intensity. The temperature effect of the MGN@PDAs was investigated with fluorescence measurement. As shown in Figure. S5, when the temperature increased, the fluorescence of MGN@PDAs also increased. A sharp intensity change occurred when the temperature exceeded 60 °C after 10 minutes of heating, which indicated the breaking of hydrogen bonds in the MGN@PDAs.

MGN@PDAs as a MRI contrast agent

MGN@PDAs could be used as a good MRI contrast agent. The capability of MGN@PDAs for T_2 imaging was investigated. All the measurements were performed on the Magnetom Avanto MRI machine (Siemens) with a constant magnetic field of 1.5 T. MRI imaging properties of PDAs, water, MGN and MGN@PDAs with different dilution solutions were explored, respectively. Figure. S6 shows the MRI T_2 images of these solutions. No obvious contrast effect was observed for PDAs, while MGN and MGN@PDAs exhibited remarkable T_2 contrast imaging effects.

Imprinting of the MGN@PDAs on different substrates

To prove the generality of the MGN@PDAs inks, different substrates, such as paper, glass, clothes,

plastics and banknotes, were utilized for MGN@PDAs ink printing. Figure. S7 shows the digital camera images of the “dragon” pattern imprinted on different substrates. The MGN@PDAs inks demonstrated good reliability and compatibility, which are essential properties for real applications.

2. Supplementary Figureures

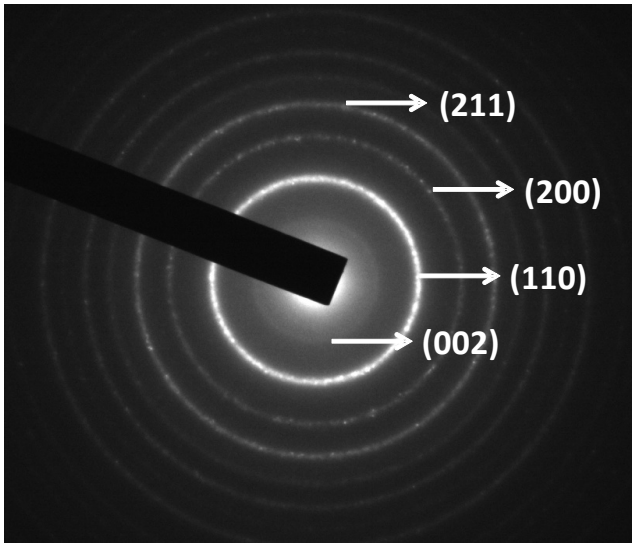

Figure. S1. Selected area electron diffraction characterization of the MGN@PDAs.

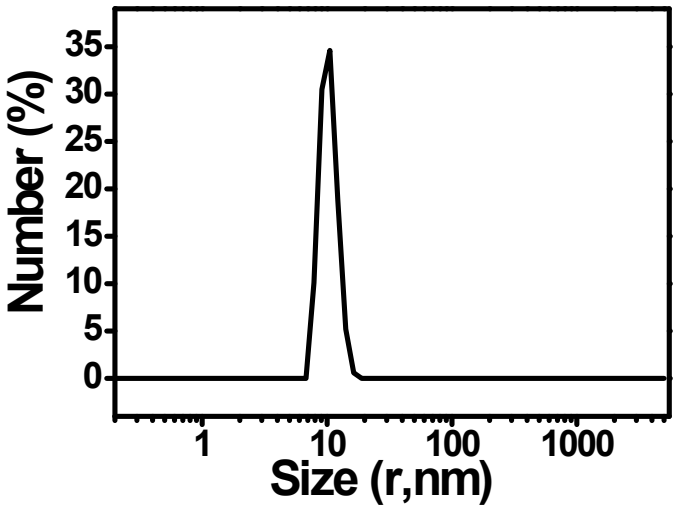

Figure. S2. DLS characterization of the size distribution of suspended MGN@PDAs.

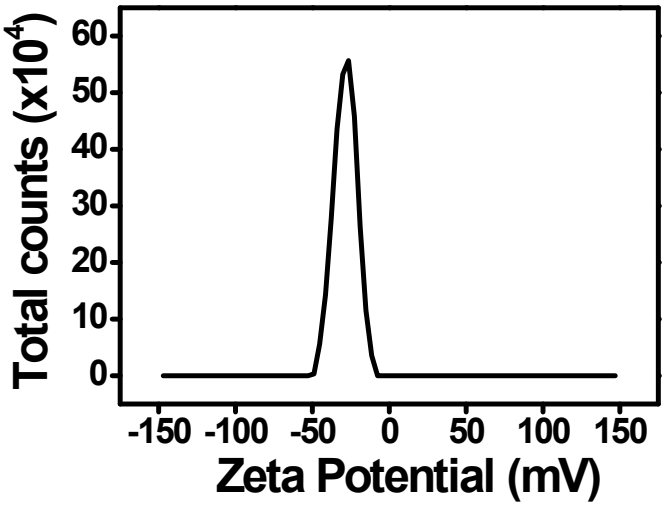

Figure. S3. Zeta potential curves of the MGN@PDAs water solution at room temperature on the ZetaSizer Nano ZS90.

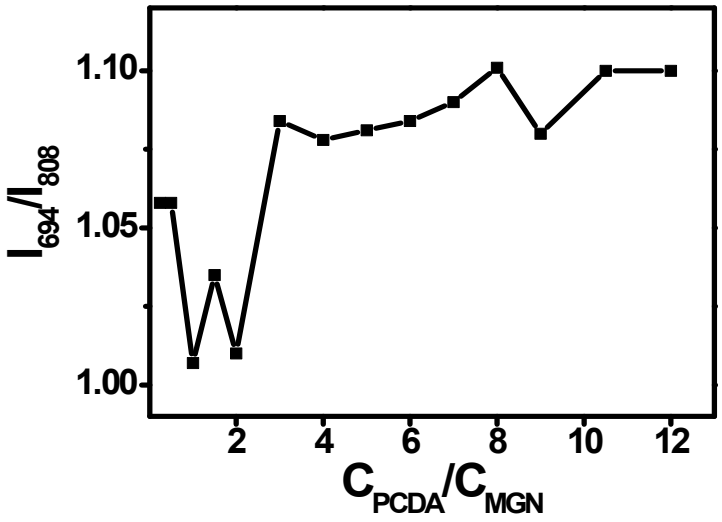

Figure. S4. Optimization of the fabrication of PCDA assembly on MGN surfaces.

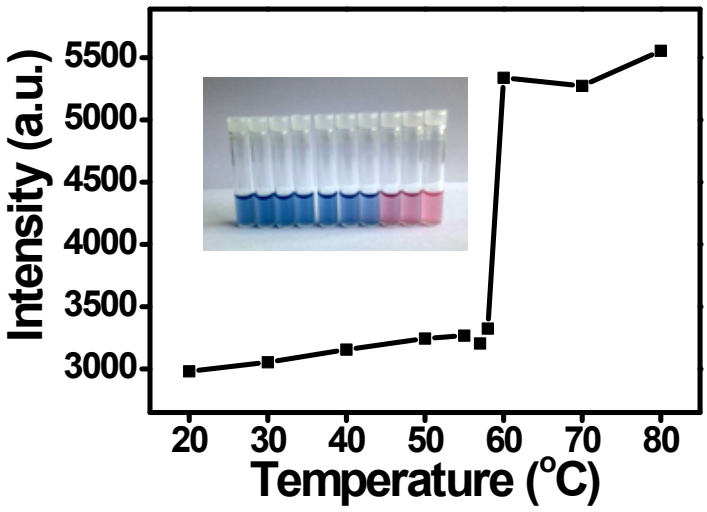

Figure. S5. Thermal heating response of MGN@PDAs. Fluorescence signal changes according to various temperatures. Inset: MGN@PDAs solutions after thermal heating to different temperatures.

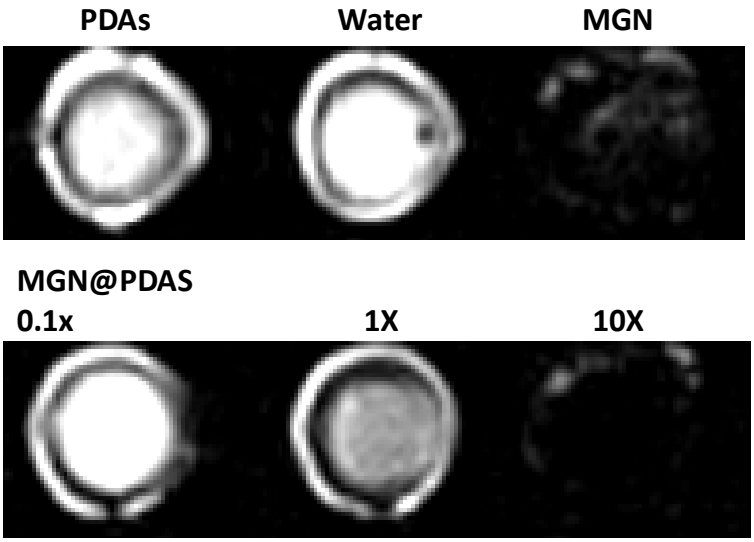

Figure. S6. MRI T_2 images of PDAs, water, MGN and MGN@PDAs solutions.

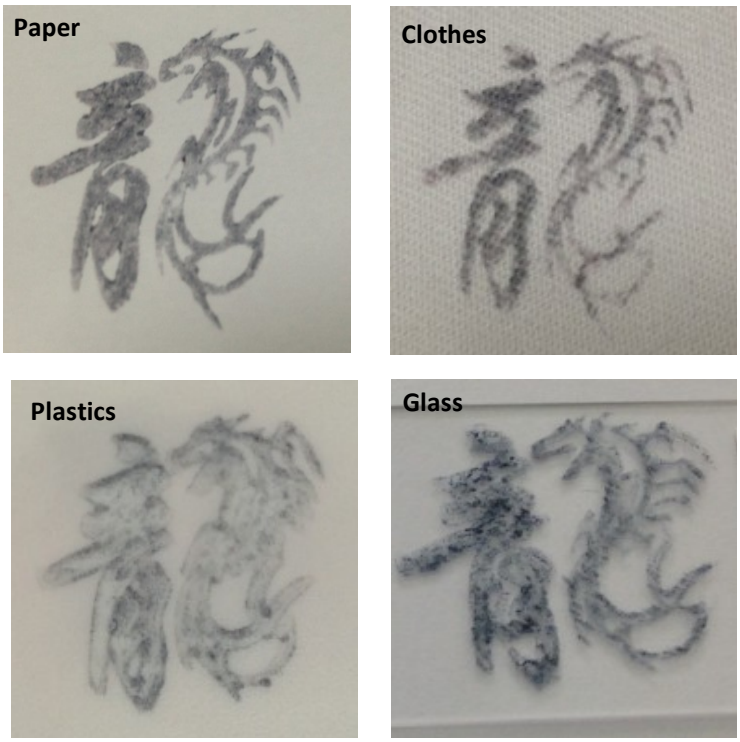

Figure. S7. Digital camera images of the "dragon" pattern imprinted on different substrates with MGN@PDAs inks.